OXFORD

LinearFold: linear-time approximate RNA folding by 5'-to-3' dynamic programming and beam search

Liang Huang[1,2,*], He Zhang[2,†], Dezhong Deng[1,†], Kai Zhao[1,‡], Kaibo Liu[1,2], David A. Hendrix[1,3] and David H. Mathews[4,5,6]

[1]School of Electrical Engineering and Computer Science, Oregon State University, Corvallis, OR 97330, USA, [2]Baidu Research USA, Sunnyvale, CA 94089, USA, [3]Department of Biochemistry & Biophysics, Oregon State University, [4]Department of Biochemistry & Biophysics, [5]Center for RNA Biology and [6]Department of Biostatistics & Computational Biology, University of Rochester Medical Center, Rochester, NY 48306, USA

*To whom correspondence should be addressed.
†The authors wish it to be known that these authors contributed equally.
‡Present address: Google, Inc, New York, NY 10011, USA.

Abstract

Motivation: Predicting the secondary structure of an ribonucleic acid (RNA) sequence is useful in many applications. Existing algorithms [based on dynamic programming] suffer from a major limitation: their runtimes scale cubically with the RNA length, and this slowness limits their use in genome-wide applications.

Results: We present a novel alternative $O(n^3)$-time dynamic programming algorithm for RNA folding that is amenable to heuristics that make it run in $O(n)$ time and $O(n)$ space, while producing a high-quality approximation to the optimal solution. Inspired by incremental parsing for context-free grammars in computational linguistics, our alternative dynamic programming algorithm scans the sequence in a left-to-right (5'-to-3') direction rather than in a bottom-up fashion, which allows us to employ the effective beam pruning heuristic. Our work, though inexact, is the first RNA folding algorithm to achieve linear runtime (and linear space) without imposing constraints on the output structure. Surprisingly, our approximate search results in even higher overall accuracy on a diverse database of sequences with known structures. More interestingly, it leads to significantly more accurate predictions on the longest sequence families in that database (16S and 23S Ribosomal RNAs), as well as improved accuracies for long-range base pairs (500+ nucleotides apart), both of which are well known to be challenging for the current models.

Availability and implementation: Our source code is available at https://github.com/LinearFold/LinearFold, and our webserver is at http://linearfold.org (sequence limit: 100 000nt).

Contact: liang.huang.sh@gmail.com

Supplementary information: Supplementary data are available at *Bioinformatics* online.

1 Introduction

Ribonucleic acid (RNA) is involved in numerous cellular processes (Eddy, 2001). The dual nature of RNA as both a genetic material and functional molecule led to the RNA World hypothesis, that RNA was the first molecule of life (Gilbert, 1986), and this dual nature has also been utilized to develop *in vitro* methods to evolve functional sequences (Joyce, 1994). Furthermore, RNA is an important drug target and agent (Angelbello *et al.*, 2018; Castanotto and Rossi, 2009; Childs-Disney *et al.*, 2007; Crooke, 2004; Gareiss *et al.*, 2008; Palde *et al.*, 2010; Sazani *et al.*, 2002).

Predicting the secondary structure of an RNA sequence, defined as the set of all canonical base pairs (A–U, G–C, G–U, see Fig. 1A), is an important and challenging problem (Hofacker and Lorenz, 2014; Seetin and Mathews, 2012). Knowing the structure reveals crucial information about the RNA's function, which is useful in many applications ranging from ncRNA detection (Fu *et al.*, 2015; Gruber *et al.*, 2010; Washietl *et al.*, 2012) to the design of oligonucleotides for knockdown of message (Lu and Mathews, 2008; Tafer *et al.*, 2008). Since experimentally determining the structure is expensive and time-consuming, and given the overwhelming increase in genomic data (about 10^{21} base-pairs per year) (Stephens *et al.*, 2015),

A

B 5′
GCGGGAAUAGCUCAGUUGGUAGAGCACGACCUUGCCAAGGUCGGGGUCGCGAGUUCGAGUCUCGUUUCCCGCUCCA 3′
((((((((..((((.........)))).(((((.......)))))…..(((((.......)))))))))))))….

1	*our linear-time heuristic algorithm scans from 5′ to 3′*	n

C

type	pair distance	time	space	systems/examples
global	unbounded	$O(n^3)$	$O(n^2)$	RNAstructure, RNAfold, …
local	$\leq L$	$O(nL^2)$	$O(nL)$	Rfold, RNAplfold, LocalFold, …
global	unbounded	$O(nb \log b)$	$O(nb)$	LinearFold (**this work**)
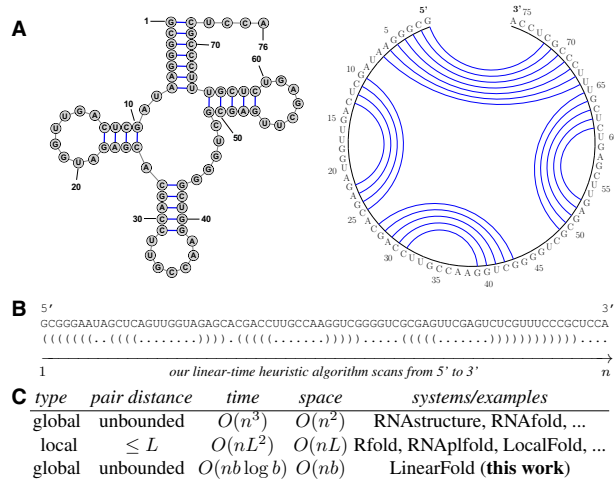
Fig. 1. Summary of our work. (**A**) Secondary structure representations of *E.coli* tRNA^{Gly}; (**B**) the corresponding dot-bracket format and an illustration of our algorithm, which scans the sequence left-to-right, and tags each nucleotide as '.' (unpaired), '(' (to be paired with a future nucleotide) or ')' (paired with a previous nucleotide). (**C**) Comparison between our work and existing ones. *L* is the limit of pair distance in local folding methods (often ≤150), and *b* is the beam size in our work (default 100). Our algorithm, though approximate, is the first to achieve linear runtime without imposing constraints on the output structure

computational methods have been widely used as an alternative to automatically predict the structure. Widely used systems such as RNAstructure (Mathews and Turner, 2006), Vienna RNAfold (Lorenz *et al.*, 2011), CONTRAfold (Do *et al.*, 2006) and CentroidFold (Sato *et al.*, 2009), all use virtually the same dynamic programming algorithm (Nussinov *et al.*, 1978; Zuker and Stiegler, 1981) to find the best-scoring (lowest free energy, maximum expected accuracy or best model score) structure (Mathews and Turner, 2006; Washietl *et al.*, 2012). However, this set of algorithms, borrowed from computational linguistics (Kasami, 1965; Younger, 1967), has a running time of $O(n^3)$ that scales *cubically* with the sequence length *n*, which is too slow for long RNA sequences (Lange *et al.*, 2012).

As an alternative, faster algorithms that predict only a restricted subset of structures have been proposed. On the one hand, local folding methods such as Rfold (Kiryu *et al.*, 2008), Vienna RNAplfold (Bernhart *et al.*, 2006) and LocalFold (Lange *et al.*, 2012) run in linear time but only predict base pairs up to *L* nucleotides apart ($L \leq 150$ in the literature; see Fig. 1C). On the other hand, due to the prohibitive cubic runtime of standard methods, it has been a common practice to divide long RNA sequences into short segments (e.g. ≤700nt) and predict structures within each segment only (Andronescu *et al.*, 2007; Licon *et al.*, 2010; Watts *et al.*, 2009). All these local methods omit long-range base pairs, which theoretical and experimental studies have demonstrated to be common in natural RNAs, especially between the 5′ and 3′ ends (Lai *et al.*, 2018; Li and Reidys, 2018; Seetin and Mathews, 2012).

We instead design *LinearFold*, an approximate algorithm that is the first in RNA folding to achieve linear runtime (and linear space) without imposing constraints on the output structure such as base pair distance. While the classical $O(n^3)$-time algorithm is bottom-up, making it hard to linearize, ours runs left-to-right (i.e. 5′-to-3′), incrementally tagging each nucleotide in the dot-bracket format (Fig. 1B). While this naive version runs in the exponential time of $O(3^n)$, we borrow an efficient packing idea from computational linguistic (Tomita, 1988) that reduces the runtime back to $O(n^3)$. This novel left-to-right $O(n^3)$ dynamic program is also a contribution of this article. Furthermore, on

top of this exact algorithm, we apply beam search, a popular heuristic to prune the search space (Huang and Sagae, 2010), which keeps only the top *b* highest-scoring (or lowest energy) states for each prefix of the input sequence, resulting in an $O(nb \log b)$ time approximate search algorithm, where *b* is the beam size chosen by the user.

Our approach can 'linearize' any dynamic programming-based pseudoknot-free RNA folding system. In particular, we demonstrate two versions of LinearFold, LinearFold-V using the thermodynamic free energy model (Mathews *et al.*, 2004) from Vienna RNAfold (Lorenz *et al.*, 2011), and LinearFold-C using the machine learned model from CONTRAfold (Do *et al.*, 2006). We evaluate our systems on a diverse dataset of RNA sequences with well-established structures, and show that while being substantially more efficient, LinearFold leads to even higher average accuracies over all families, and more interestingly, LinearFold is significantly more accurate than the exact search methods on the longest families, 16S and 23S Ribosomal RNAs. In addition, LinearFold is also more accurate on long-range base pairs, which is well known to be a challenging problem for the current models (Amman *et al.*, 2013).

Finally, our work establishes a new connection among computational linguistics, compiler theory and RNA folding (see Supplementary Fig. SI 7).

2 The LinearFold algorithm

2.1 Problem formulation

Given an RNA sequence $\mathbf{x} = x_1 x_2 \ldots x_n$, where each $x_i \in \{\mathbf{A}, \mathbf{C}, \mathbf{G}, \mathbf{U}\}$, the secondary structure prediction problem aims to find the best-scoring pseudoknot-free structure $\hat{y}$ by maximizing a scoring function $sc_{\mathbf{w}}$ (e.g. model score or negative free energy) where $\mathbf{w}$ are the model parameters:

$$\hat{y} = \underset{y \in \mathcal{Y}(\mathbf{x})}{\textbf{argmax}}\, sc_{\mathbf{w}}(\mathbf{x}, y). \tag{1}$$

Here $\mathcal{Y}(\mathbf{x})$ is the set of all possible pseudoknot-free secondary structures for input $\mathbf{x}$ of length *n*

$$\left\{ y \in \{., (\ , \ )\}^n \mid \text{balanced}(y), \text{valid}(\mathbf{x}, \text{pairs}(y)) \right\}$$

where balanced(y) checks if y has balanced brackets, valid($\mathbf{x}$, pairs(y)) checks if all pairs in y are valid (CG, AU, GU), and pairs(y) returns the set of (i, j) pairs where x_i and x_j form a base pair in y, e.g. pairs("((.))") = $\{(1, 5), (2, 4)\}$. See Supplementary section A for detailed definitions.

All dynamic programming-based prediction algorithms, including ours, require the scoring function $sc_{\mathbf{w}}(\mathbf{x}, \cdot)$ to *decompose* to smaller structures. For simplicity of presentation, in the main text we will use a very simple decomposition to individual pairs and unpaired nucleotides:

$$sc_{\mathbf{w}}(\mathbf{x}, y) = \sum_{(i,j) \in \text{pairs}(y)} w_{x_i x_j} + \sum_{i \in \text{unpaired}(y)} w_{\text{unpaired}} \tag{2}$$

In this framework, we can assign different scores for different pairs, and incur a penalty for each unpaired nucleotide. For the example in Figure 2, we simply set $w_{\text{CG}} = w_{\text{AU}} = w_{\text{GU}} = 1$ and $w_{\text{unpaired}} = -0.1$; therefore, $sc_{\mathbf{w}}$("CCAGG", "((.))") = $2w_{\text{CG}} + w_{\text{unpaired}} = 1.9$.

In reality, however, the actual scoring functions used by CONTRAfold, RNAfold, and our LinearFold are much more complex, and they decompose into individual loops. See Supplementary section B for details.
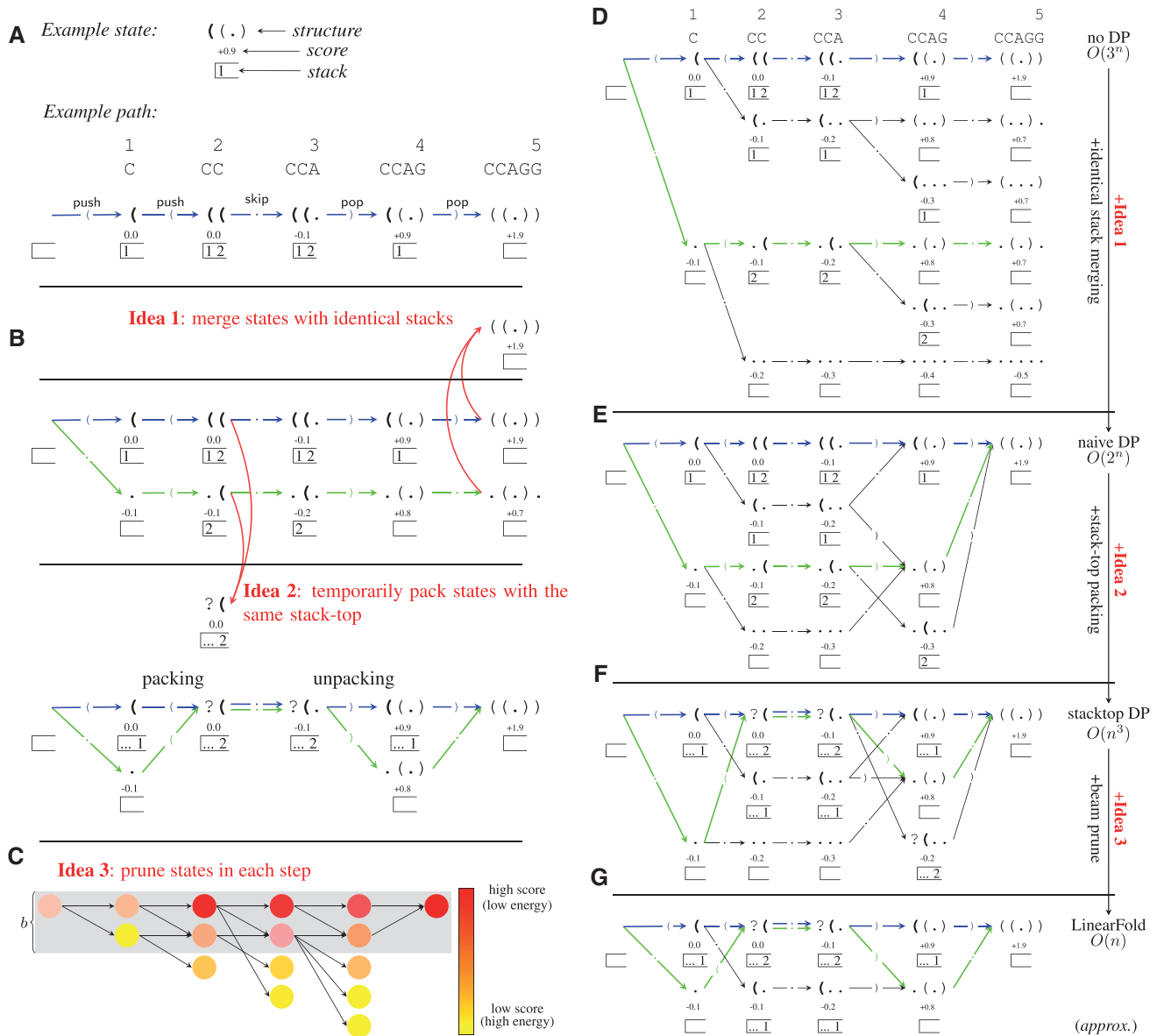
Fig. 2. Illustration of the LinearFold approach, using a short sequence CCAGG and the simple scoring function ([Eq. 2](#)). (**A**) An example state and an example (actually optimal) path, showing states (predicted prefix structures), actions (*push* '(', *skip* '.', and *pop* ')'), and stacks (unpaired open brackets, which are shown in bold in states). (**B**) Two example paths (the optimal one in blue and a suboptimal one in green) and two essential ideas of left-to-right dynamic programming: merging equivalent states with identical stacks (Idea 1) and packing temporarily equivalent states sharing the same stack top, and corresponding unpacking upon *pop* (Idea 2). (**C**) Illustration of beam search, which keeps top *b* states (those in the shaded region) per step (Idea 3). (**D**) The whole search space of the naive algorithm ($O(3^n)$ time). (**E**) Improving to $O(2^n)$ time with Idea 1. (**F**) Further improving to $O(n^3)$ time with Idea 2. (**G**) Further improving to $O(n)$ time (but with approximate search) with Idea 3. In B, F, and G, each green/blue arrow pair ?(⊏⟶⊐?(. is actually a single arrow, denoting two paths temporarily packed as one; we draw paired arrows to highlight that two states .(and ((are performing *skip* action together. Note the version up to Idea 2 is exact and worst-case $O(n^3)$ time

2.2 Idea 0: Brute-force search: $O(3^n)$

The initial idea, introduced in [Figure 1B](#), is to scan the RNA sequence left-to-right, maintaining a *stack* along the way, and performing one of the three actions (push, skip or pop) at each step. More formally, we denote each *state* at step j ($j = 0 \ldots n$) as a tuple along with a score s:

$$\langle y, \sigma, j \rangle : s,$$

where y is the (sub)structure for the prefix $x_1 \ldots x_j$, and σ is the stack consisting of unmatched opening bracket positions in y. For example, in Step 4, if $y = $ '((.)', then $\sigma = [1]$ and $s = 0.9$ (see [Fig. 2A](#)); note that we denote open brackets in bold. Each state at

step j can transition into a subsequent state of step $j + 1$, taking one of the three actions:

1. *push*: label x_{j+1} as '(' for it to be paired with a downstream nucleotide, and pushing $j + 1$ on to the stack, notated:

$$\frac{\langle y, \sigma, j \rangle : s}{\langle y \circ \text{'(', } \sigma | (j+1), j+1 \rangle : s}$$

2. *skip*: label x_{j+1} as '.' (unpaired and skipped):

$$\frac{\langle y, \sigma, j \rangle : s}{\langle y \circ \text{'.', } \sigma, j+1 \rangle : s + w_{\text{unpaired}}}$$

3. *pop*: label x_{j+1} as ')', paired with the upstream nucleotide x_i where i is the top of the stack, and pop i (if $x_i x_{j+1}$ pair is allowed):

$$\frac{\langle \mathbf{y}, \sigma | i, j \rangle : s}{\langle \mathbf{y} \circ ')', \sigma, j+1 \rangle : s + w_{x_i x_{j+1}}}$$

We start with the init state $\langle '', [], 0 \rangle : 0$ and finish with any state $\langle \mathbf{y}, [], n \rangle : s$ with an empty stack (ensuring the output is a well-balanced dot-bracket sequence). See Figure 2A for an example path for input sequence CCAGG, and Figure 2D for all valid paths.

The above procedure describes a naive exhaustive search without dynamic programming which has exponential runtime $O(3^n)$, as there are up to three actions per step (see Fig. 2D).

Next, Figure 2B sketches the two key dynamic programming ideas that speed up this algorithm to $O(n^3)$ by merging and packing states.

2.3 Idea 1: merge states with identical stacks: $O(2^n)$

We first observe that different states can have the same stack; for example, in Step 5, both '.(.).' and '((.))' have the same empty stack (see Fig. 2B, Idea 1); and in step 4, both '(. .' and '((.' have the same stack [1] (see Fig. 2D). These states can be merged, because even though they have different histories, going forward they are exactly equivalent. After merging we save the state with the highest score and discard all others which have no potential to lead to the optimal structure. More formally, we merge two states with the same stack:

$$\left. \begin{array}{c} \langle \mathbf{y}, \sigma, j \rangle : s \\ \langle \mathbf{y}', \sigma, j \rangle : s' \end{array} \right\} \rightarrow \langle \sigma, j \rangle : \langle \mathbf{y}'', s'' \rangle$$

where

$$\langle \mathbf{y}'', s'' \rangle = \begin{cases} \langle \mathbf{y}, s \rangle & \text{if } s > s' \\ \langle \mathbf{y}', s' \rangle & \text{otherwise} \end{cases}$$

This algorithm is faster but still has exponential $O(2^n)$ time as there are exponentially many different stacks (see Fig. 2E).

2.4 Idea 2: pack temporarily equivalent states: $O(n^3)$

We further observe that even though some states have different stacks, they might share the same stack top. For example, in step 2, '.(' and '((' have [2] and [1, 2] as their stacks, resp., but with the same stack top 2. Our key insight is that two states with the same stack-top are 'temporarily equivalent' and can be 'packed' as they would behave equivalently until the stack-top open bracket is closed (i.e. matched), after which they 'unpack' and diverge. As shown in Fig. 2B (Idea 2), both '.(' and '((' are looking for a 'G' to match with the stack top x_2='C', and can be packed as '?(' with stack [. . .2] where '?' and '. . .' represent histories that are not important for now. After skipping the next nucleotide x_3='A', they become '?(.' and upon matching the next nucleotide x_4='G' with the stack-top x_2='C', they unpack, resulting in '.(.)' and '((.)'.

More formally, two states $\langle \sigma | i, i \rangle : \langle \mathbf{y}, s \rangle$ and $\langle \sigma' | i, i \rangle : \langle \mathbf{y}', s' \rangle$ sharing the same stack top can be packed:

$$\left. \begin{array}{c} \langle \sigma | i, i \rangle : \langle \mathbf{y}, s \rangle \\ \langle \sigma' | i, i \rangle : \langle \mathbf{y}', s' \rangle \end{array} \right\} \rightarrow \langle i, i \rangle : \langle (, 0 \rangle$$

Note that (i) we only need two indices to index the packed state; (ii) we omit the ?'s since they contain no information; and (iii) somewhat counterintuitively, the resulting packed state's (sub)structure and score, $\langle (, 0 \rangle$ do not depend on the original states before packing.

More formally, for any packed state $\langle i, j \rangle : \langle \mathbf{y}, s \rangle$, its $\mathbf{y}$ is a substructure only for the substring $x_i \dots x_j$, and its score s is also for that portion only, i.e. $s = sc_\mathbf{w}(x_i \dots x_j, \mathbf{y})$. We can grow it by skip

$$\frac{\langle i, j \rangle : \langle \mathbf{y}, s \rangle}{\langle i, j+1 \rangle : \langle \mathbf{y} \circ '.', s + w_{\text{unpaired}} \rangle}$$

or push actions

$$\frac{\langle i, j \rangle : \langle \mathbf{y}, s \rangle}{\langle j+1, j+1 \rangle : \langle (, 0 \rangle}.$$

The pop action is more involved. If x_i and x_{j+1} match, we pop i, but where can we find the 'previous stack top'? It is *not* specified in the packed state. Therefore, we need to find a state $\langle k, i-1 \rangle : \langle \mathbf{y}', s' \rangle$ that combines with the current state:

$$\frac{\langle k, i-1 \rangle : \langle \mathbf{y}', s' \rangle \quad \langle i, j \rangle : \langle \mathbf{y}, s \rangle}{\langle k, j+1 \rangle : \langle \mathbf{y}' \circ \mathbf{y} \circ ')', s' + s + w_{x_i x_{j+1}} \rangle}$$

This version (see Fig. 2F) runs in worst-case $O(n^3)$ time, because the pop step involve three free indices. It guarantees to return the optimal-scoring structure. It is inspired by a well-established algorithm in natural language parsing (Huang and Sagae, 2010; Tomita, 1988); see Supplementary Figure SI 7. Although this $O(n^3)$ runtime is the same as those classical bottom-up ones, its unique left-to-right nature makes it amenable to $O(n)$ beam search.

2.5 Idea 3 (approximate search): beam pruning: $O(n)$

We further employ beam pruning (Huang *et al.*, 2012), a popular heuristic widely used in computational linguistics, to reduce the complexity from $O(n^3)$ to $O(n)$, but with the cost of exact search. Basically, at each step j, we only keep the b top-scoring (lowest-energy) states and prune the other, less promising, ones (because they are less likely to be part of the optimal final structure). This results in an approximate search algorithm in $O(nb^2)$ time, depicted in Figure 2C and G. On top of beam search, we borrow k-best parsing (Huang and Chiang, 2005) to reduce the runtime to $O(nb \log b)$. Here, the beam size b is a small constant (by default 100) so the overall runtime is linear in n. We will show that our approximate search achieves even higher overall accuracy than the classical exact search methods. The space complexity is $O(nb)$. See Supplementary Figure SI 6 for the real system. There are two minor restrictions in our real system: the length of an interior loop is bounded by $30nt$ (a standard limit found in most existing RNA folding software such as CONTRAfold), so is the leftmost (5'-end) unpaired segment of a multiloop (new constraint). These conditions are valid for 37°C, and no violations were found in the ArchiveII dataset.
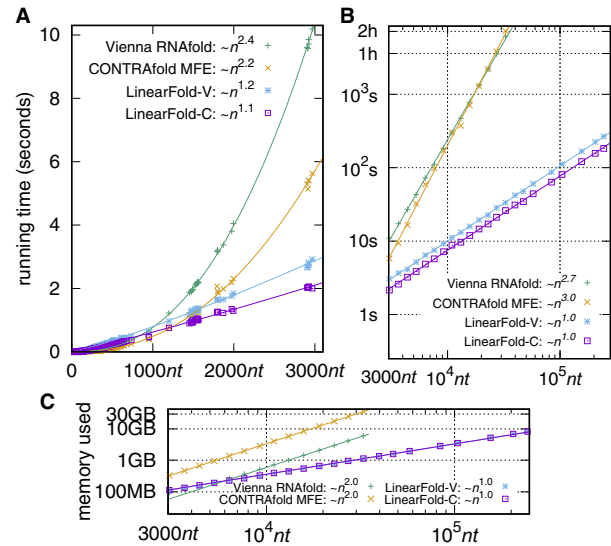
3 Results

3.1 Efficiency and scalability

We compare LinearFold's efficiency with classical cubic-time algorithms represented by CONTRAfold (Version 2.02) and Vienna RNAfold (Version 2.4.10) (http://contra.stanford.edu/ and https://www.tbi.univie.ac.at/RNA/download/sourcecode/2_4_x/ViennaRNA-2.4.10.tar.gz). We use two datasets: (i) the ArchiveII dataset (Sloma and Mathews, 2016), a diverse set of RNA sequences with known structures (http://rna.urmc.rochester.edu/pub/archiveII.tar.gz; we removed those sequences found in the S-Processed set, see Supplementary Table SI 1 for details), and (ii) a sampled subset of RNAcentral (The RNAcentral Consortium, 2017) (https://rnacentral.

org/), a comprehensive set of ncRNA sequences from many databases. While ArchiveII contains sequences of 3000*nt* or less, RNAcentral has many much longer ones, with the longest being 244 296*nt* (Homo Sapiens Transcript NONHSAT168677.1, from the NONCODE database (Zhao *et al.*, 2016)). We run all programs (compiled by GCC 4.9.0) on Linux, with 3.40GHz Intel Xeon E3-1231 CPU and 32G memory.

Figure 3A shows that on the relatively short ArchiveII set, LinearFold's runtime scales almost linearly with the sequence length, while the two baselines have superquadratic runtimes. On the much longer RNAcentral set, Figure 3B shows strictly linear
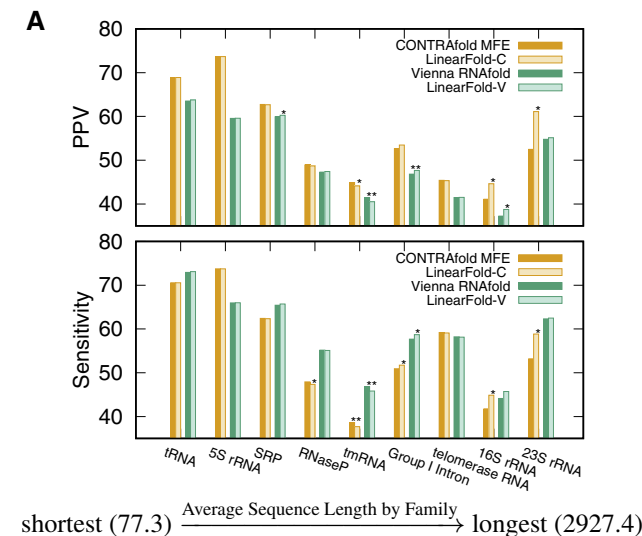
runtime for LinearFold and near-cubic runtimes for the baselines, which agrees with the asymptotic analyses and suggests that the minor deviations from the theoretical runtimes are due to the short sequence lengths in the ArchiveII set. For a sequence of $\sim$10 000*nt* (e.g. the HIV genome), LinearFold takes only 8 s, while the baselines take 4 min. For a sequence of 32 753*nt*, LinearFold takes 26 s, while CONTRAfold and RNAfold take 2 and 1.7 h, respectively.

In addition, LinearFold uses only $O(n)$ memory (Fig. 3C). The classical $O(n^3)$-time algorithm uses $O(n^2)$ space, because it needs to solve the best-scoring substructure for each substring $[i, j]$ bottom-up. LinearFold, in contrast, uses $O(n)$ space thanks to left-to-right beam search, and is the first $O(n)$-space algorithm to be able to predict base pairs of unbounded distance. It is able to fold the longest sequence in RNAcentral (244 296*nt*) within 3 min, while neither CONTRAfold or RNAfold runs on anything longer than 32 767*nt* due to datastructure limitations. As a result, the sequence limit on our web server (10^5*nt*, see abstract) is 10$\times$ that of RNAfold web server (the previous largest), being by far the largest limit among all available servers (as of March 2019). The curve-fittings in Figure 3 were done log-log in gnuplot with $n > 10^3$ in A, $n > 3 \times 10^3$ in B, and $n > 10^4$ in C, to focus on the asymptotics.

3.2 Accuracy

We next compare LinearFold with the two baselines in accuracy, reporting both positive predictive value (PPV, the fraction of predicted pairs in the known structure) and sensitivity (the fraction of known pairs predicted) on each RNA family in the ArchiveII dataset, allowing correctly predicted pairs to be offset by one position for one nucleotide as compared to the known structure (Sloma and Mathews, 2016); we also report exact match accuracies in Supplementary Table SI 2. We test statistical significance using a paired, one-sided permutation test, following (Aghaeepour and Hoos, 2013).

Figure 4 shows that LinearFold is more accurate than the baselines, and interestingly, this advantage is more pronounced on longer sequences. Individually, LinearFold-C (the LinearFold implementation of the

Fig. 3. Efficiency and scalability of LinearFold. (**A**) Runtime comparisons on the ArchiveII dataset with the two baselines, CONTRAfold MFE and Vienna RNAfold. (**B**) Runtime comparisons on the RNAcentral dataset (log–log). (**C**) Memory usage comparisons (RNAcentral set, log–log). LinearFold uses $O(n)$ time and memory, being substantially faster and slimmer than the $O(n^3)$-time, $O(n^2)$-space, baselines on long sequences

Overall	PPV	Sensitivity
CONTRAfold MFE	54.51	55.36
LinearFold-C	55.84 (+1.3)	56.24 (+0.9)
Vienna RNAfold	50.22	58.74
LinearFold-V	50.51 (+0.3)	58.97 (+0.2)

Fig. 4. Accuracy of LinearFold. (**A**) Each bar represents PPV/sensitivity averaged over all sequences in one family. Statistical significance is marked as $*(0.01 \leq P < 0.05)$ or $**(P < 0.01)$. See Table 2 for details. (**B**) The overall accuracies, averaging over all families. (**C**) Each bar represents the overall PPV/sensitivity of all base pairs in a certain length range across all sequences. Supplementary Figure SI 1. shows a similar result for LinearFold-V. Overall, LinearFold outperforms exact search baselines, especially on longer families and long-range pairs

CONTRAfold model) is significantly more accurate in sensitivity than CONTRAfold on one family (Group I Intron), and both PPV/sensitivity on two families (16S and 23S ribosomal RNAs), with the last two being the longest families in this dataset, where they have average lengths 1548*nt* and 2927*nt*, and enjoyed +3.56%/+3.09% and +8.65%/+5.66% (absolute) improvements in PPV/sensitivity, respectively. LinearFold-V (the LinearFold implementation of the Vienna RNAfold model) also outperforms RNAfold with significant improvements in PPV on two families (SRP and 16S rRNA), and both PPV/sensitivity on one family (Group I Intron). Overall (across all families), LinearFold-C outperforms CONTRAfold by +1.3%/+0.9% PPV/sensitivity, while LinearFold-V outperforms RNAfold by +0.3%/+0.2%. See Supplementary Table SI 1 for details.

Long-range base pairs are notoriously difficult to predict under current models (Amman *et al.*, 2013). Interestingly, LinearFold is more accurate in both PPV and sensitivity than the exact search algorithm for long-range base pairs of nucleotides greater than 500 nucleotides apart, as shown in Figure 4C. Combined with Supplementary Figure SI 1, we conclude that LinearFold is more selective in predicting long-range base pairs (higher PPV), but nevertheless predicts *more* such pairs that are correct (higher Sensitivity). Supplementary Figure SI 2B and C further shows that both LinearFold-C and LinearFold-V correct the severe overprediction of those long-range base pairs in exact search baselines.

Interestingly, even though our algorithm scans 5′-to-3′, the accuracy does not degrade toward the 3′-end, shown in Supplementary Figure SI 4.

3.3 Search quality

Above we used beam size 100. Now we investigate the impacts of varying beam size. We first study its impact on search quality. Since our search is approximate, we quantify the notion of *search error* (Huang and Sagae, 2010) as the difference in score or free energy between $\hat{y}$, the optimal structure returned by exact search, and $\bar{y}$, the one found by our linear-time beam search, i.e.

$$sc_{\mathbf{w}}(\mathbf{x}, \hat{y}) - sc_{\mathbf{w}}(\mathbf{x}, \bar{y}).$$

The smaller this gap, the better the search quality. Figure 5A shows that search error shrinks with beam size, quickly converging to 0 (exact search); Figure 5B–C show that the search error (at $b = 100$) grows linearly with sequence length, indicating that our search quality does not degrade with longer sequences (the average search error per nucleotide stays the same).

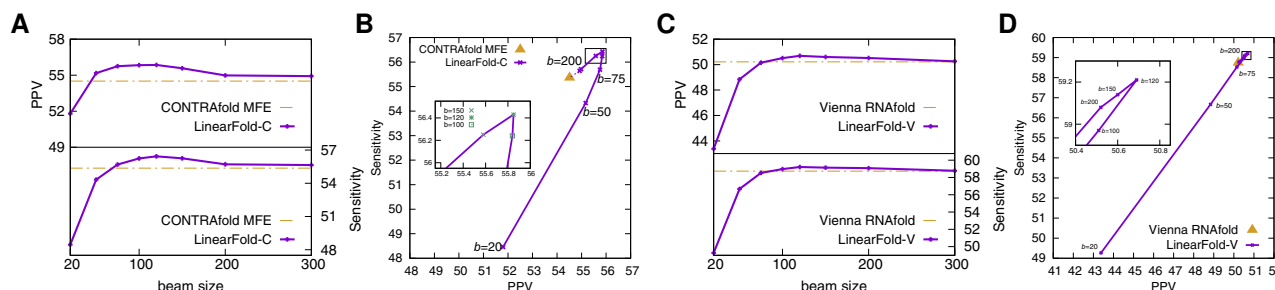### 3.4 Impacts of beam size on prediction accuracy

Figure 6A plots PPV and sensitivity as a function of beam size. LinearFold-C outperforms CONTRAfold MFE in both PPV and sensitivity with $b \geq 75$ and is stable with $b \in [100, 150]$. Figure 6B shows the tradeoff between PPV and sensitivity. Both PPV and sensitivity increase initially with beam size, culminating at $b = 120$, and then decrease, converging to exact search. We do not tune the beam size on any dataset and use the round number of 100 as default. Figure 6C–D shows a similar trend for LinearFold-V.

3.5 Example predictions: Group I intron, 16S & 23S rRNAs

Figure 7 visualizes the predicted secondary structures from three RNA families: *Cryptothallus mirabilis* Group I Intron, *Bacillus subtilis* 16S rRNA and *Escherichia coli* 23S rRNA. We observe that LinearFold substantially reduces false positives (shown in red), especially on the CONTRAfold model. It also correctly predicts many
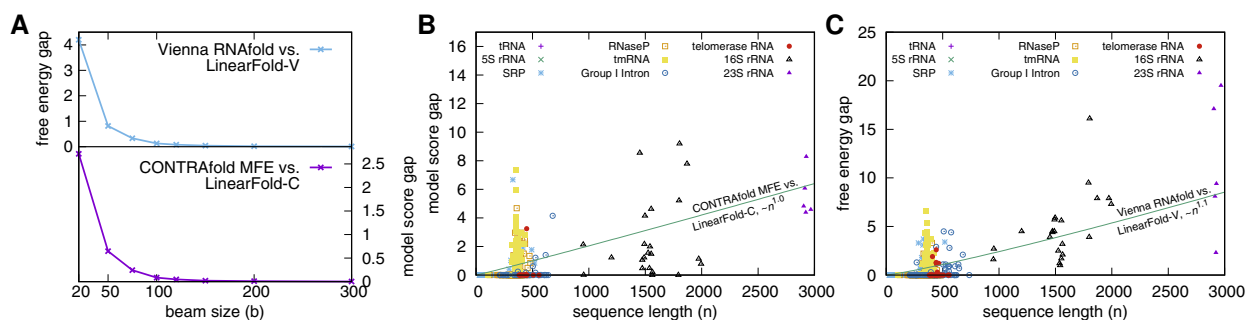

Fig. 5. Search error (model score gap or free energy gap $\Delta\Delta G$). (**A**) Average free energy gap (Vienna RNAfold vs. LinearFold-V) and model cost gap (CONTRAfold vs. LinearFold-C) with varying beam size; the search error shrinks with beam size, quickly converging to 0. (**B** and **C**) The search error (or gap) grows linearly with sequence length. Here, tmRNA is the outlier with disproportionally severe search errors, which can explain the slightly worse accuracies of LinearFold on tmRNA in Figure 4A. See Supplementary Figure SI 3. for a close-up on short sequences

Fig. 6. Impacts of beam size on prediction accuracy. (**A** and **C**) PPV and sensitivity with varying beam size for LinearFold-C (A) and LinearFold-V (C); (**B** and **D**) PPV-sensitivity tradeoff for LinearFold-C (B) and LinearFold-V (D). Note that LinearFold with $b = \infty$ is exact search in $O(n^3)$ time (Idea 2) and produces identical results to the baselines
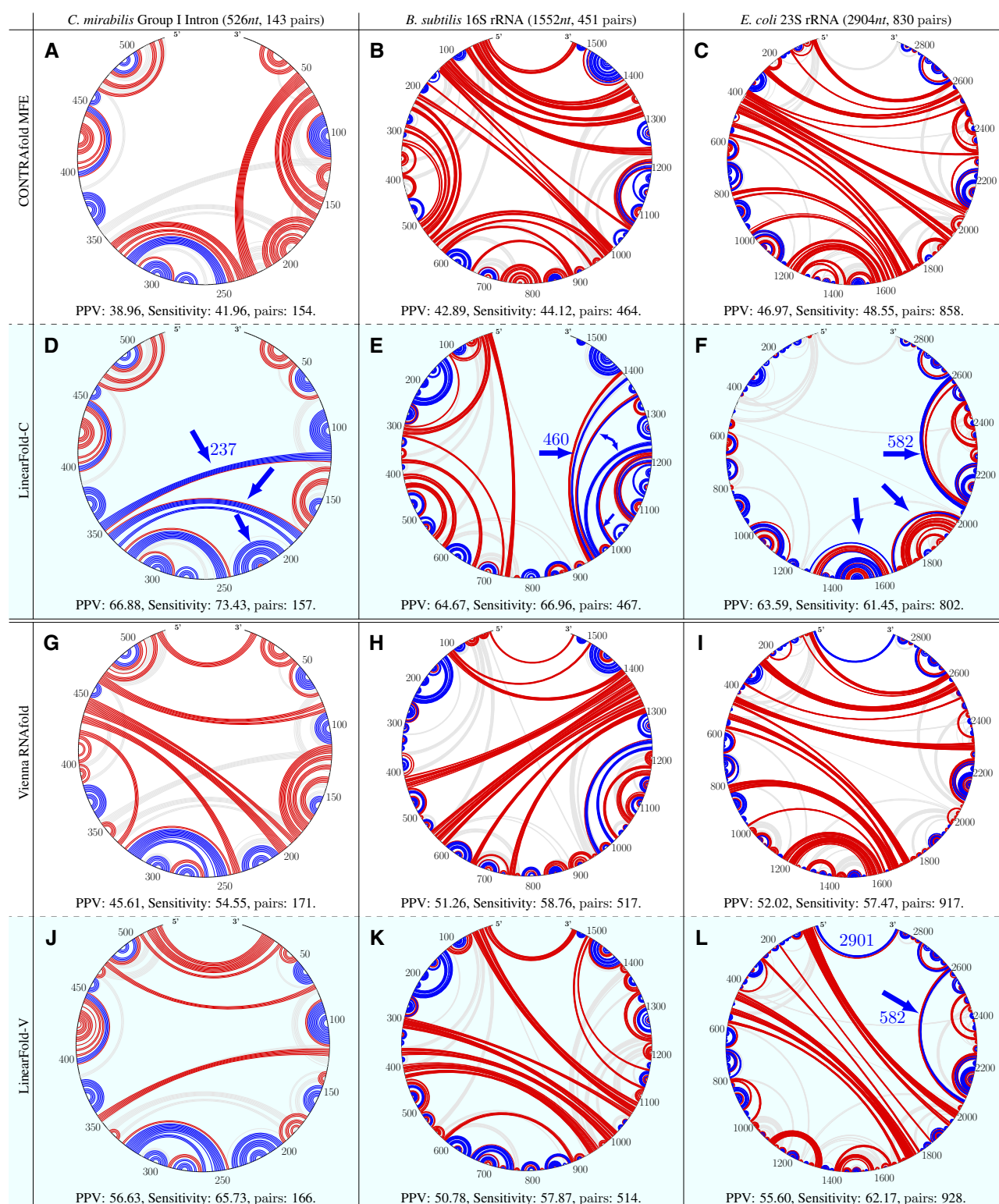
Fig. 7. Circular plots of the prediction results on three RNA sequences (from three different RNA families) comparing the baselines (A–C: CONTRAfold MFE; G–I: Vienna RNAfold) and our LinearFold (D–F: LinearFold-C; J–L: LinearFold-V). Correctly predicted base pairs are in blue (true positives), incorrectly predicted pairs in red (false positives) and missing true base pairs in light gray (false negatives). Each plot is clockwise from 5′ to 3′. We can observe that (i) our LinearFold greatly reduces the false positives, especially on CONTRAfold; (ii) our LinearFold correctly predicts many long-range pairs, e.g. LinearFold-C on all three sequences and LinearFold-V on *E.coli* 23S rRNA(L); (iii) our LinearFold is able to predict the longest 5′–3′ pairs, even with the beam size of 100, which is an order of magnitude smaller than the sequence lengths of 16S and 23S rRNAs. (iv) In almost all cases (except for LinearFold-V on *B.subtilis* 16S rRNA(K)), LinearFold substantially outperforms the corresponding baseline
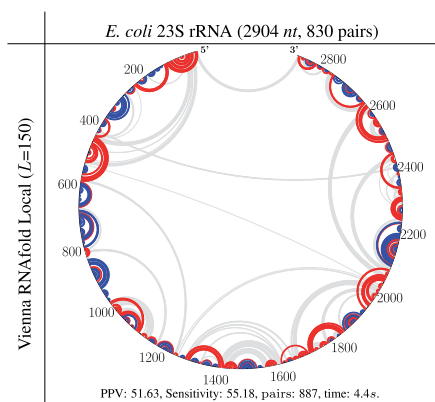
Fig. 8. Circular plots of prediction results using the local folding mode of Vienna RNAfold (which only predicts local pairs no more than 150nt apart) on the *E.coli* 23S rRNA (corresponding to Fig. 7I). Moreover, the $O(nL^2)$-time local folding (with default $L = 150$) is twice as slow as the $O(nb \log b)$-time LinearFold-V (with default $b = 100$)

(clusters of) long-range base pairs (true positives, shown in blue), e.g. in *C.mirabilis* Group I Intron with LinearFold-C (Fig. 7D, pair distance 237nt), *B.subtilis* 16S rRNA with LinearFold-C (Fig. 7E, pair distance 460nt), *E.coli* 23S rRNA with both LinearFold-C and LinearFold-V (Fig. 7F and L, pair distance 582nt). This reconfirms LinearFold's advantage in predicting long-range base pairs shown in Figure 4C. Moreover, LinearFold is able to predict the longest $5'$–$3'$ pairs, as shown in *E. coli* 23S rRNA with LinearFold-V (Fig. 7L, pair distance 2901nt). In most cases (except LinearFold-V on *B. subtilis* 16S rRNA, Fig. 7K), LinearFold improves substantially over the corresponding baselines. By contrast, local folding methods do not predict any long-range pairs, shown in Fig. 8. We use `RNAfold -maxBPspan 150` for local folding, and this limit of 150 is the largest default limit in the local folding literature and softwares.

4 Discussion

There are several reasons why our beam search algorithm, though approximate, outperforms the exact search baselines in terms of accuracy (esp. in 16S and 23S rRNAs and long-range base pairs).

1. First, the scoring functions are imperfect, so it is totally possible for a suboptimal structure (in terms of model score or free energy) to be more accurate than the optimal-score structure. For example, it was well-studied that while the lowest free energy structure contains only 72.9% of the actual base pairs (given a dataset), a structure containing 86.1% of them can be found with a free energy within 4.8% of the optimal structure (Mathews *et al.*, 1999; Zuker *et al.*, 1991).
2. Secondly, the beam search algorithm prunes lower-scoring (sub)-structures at each step, requiring the surviving (sub)structures and the final result to be highly scored for each prefix. Our results suggest that this extra constraint, like 'regularization', could compensate for the inaccuracy of the (physical or machine-learning) model, as LinearFold *systematically* picks a more accurate suboptimal structure without knowing the ground truth; indeed, this seemingly surprising phenomenon has been observed before in computational linguistics (Huang and Sagae, 2010) which inspired this work.
3. Finally, our LinearFold algorithm resembles cotranscriptional folding where RNA molecules start to fold immediately before

being fully transcribed (Gultyaev *et al.*, 1995; Meyer and Miklós, 2004). This is analogous to psycholinguistic evidence that humans incrementally parse a sentence before it is fully read or heard (Frazier and Rayner, 1982). We hypothesize that some RNA sequences have evolved to fold co-transcriptionally (Meyer and Miklós, 2004), thus making our $5'$-to-$3'$ incremental approach more accurate than bottom-up baselines. Supplementary Figure SI 5B shows a slight preference for $5'$-to-$3'$ order over $3'$-to-$5'$.

There are other algorithmic efforts to speed up RNA folding, including an $O(n^3 / \log n)$ algorithm using the Four-Russians method (Venkatachalam *et al.*, 2014), and two other sub-cubic algorithms inspired by fast matrix multiplication and context-free parsing (Bringmann *et al.*, 2016; Zakov *et al.*, 2011). We note that all of them are based on the classical cubic-time bottom-up algorithm, and thus orthogonal to our left-to-right approach. There also exists a linear-time algorithm (Rastegari and Condon, 2005) to analyze a *given* structure, but not to predict one *de novo*.

5 Conclusion and future work

We designed an $O(n)$-time, $O(n)$-space, approximate search algorithm, using incremental dynamic programming plus beam search, and apply this algorithm to both machine-learned and thermodynamic models. Besides the linearity in both time and memory (Fig. 3), we also found:

1. Though LinearFold uses only a fraction of time and memory compared with existing algorithms, our predicted structures are even more accurate overall in both PPV and sensitivity and on both machine-learned and thermodynamic models (see Fig. 4).
2. The accuracy improvement of LinearFold is more pronounced on longer families such as 16S and 23S rRNAs (see Figs 4 and 7).
3. LinearFold is also more accurate than the baselines at predicting long-range base pairs over 500nt apart (Fig. 4C), which is well known to be challenging for the current models (Amman *et al.*, 2013).
4. Although the performance of LinearFold depends on the beam size b, the number of base pairs and the accuracy of prediction are stable when b is in the range of 100–200.

There is a crucial difference between our LinearFold and local folding algorithms (Bernhart *et al.*, 2006; Kiryu *et al.*, 2008; Lange *et al.*, 2012) that can only predict pairs up to a certain distance. Theoretical and empirical studies found several evidences that *unboundedly* long-distance pairs are actually quite common in natural RNA structures: (i) the length of the longest base pair grows nearly linearly with sequence length n (Li and Reidys, 2018); (ii) the physical distance between the $5'$–$3'$ ends in folded structures is short and nearly constant (Lai *et al.*, 2018; Leija-Martínez *et al.*, 2014; Yoffe *et al.*, 2011).

Our work has several potential extensions.

1. It is possible that LinearFold can be extended to calculate the partition function and base pair probabilities for natural RNA sequences with well-defined structures, since the classical method for that task, the McCaskill (1990) algorithm, is isomorphic in structure to the cubic-time algorithms that are used as baselines in this article.
2. This linear-time approach to calculate base pair probabilities should facilitate the linear-time identification of pseudoknots, by either replacing the cubic-time McCaskill algorithm with a

linear-time one in those heuristic pseudoknot-prediction programs (Bellaousov and Mathews, 2010; Sato *et al.*, 2011), or linearizing a supercubic-time dynamic program for direct prediction with pseudoknots (Dirks and Pierce, 2003; Reeder and Giegerich, 2004).

3. We will test the hypothesis that our beams potentially capture cotranscriptional folding with empirical data on cotranscriptional folding (Watters *et al.*, 2016).

4. Being linear-time, LinearFold also facilitates faster parameter training than the cubic-time CONTRAfold using structured prediction methods (Huang *et al.*, 2012), and we envision a more accurate LinearFold using a model tailored to its own search.

Author contributions

L.H. conceived the idea and directed the project. L.H., D.D. and K.Z. designed algorithms. L.H. and D.D. wrote a Python prototype, and K.Z., D.D. and H.Z. wrote the fast C++ version. D.H.M. and D.H. guided the evaluation that H.Z. and D.D. carried out. L.H., D.D. and H.Z. wrote the manuscript; D.H.M. and D.H. revised it. K.L. made the webserver.

References

Aghaeepour,N. and Hoos,H.H. (2013) Ensemble-based prediction of RNA secondary structures. *BMC Bioinformatics*, **14**, 1.

Amman,F. *et al.* (2013) The trouble with long-range base pairs in RNA folding. In: Setubal,J.C. and Almeida,N.F. (eds) *Proceedings of the 8th Brazilian Symposium on Bioinformatics, BSB 2013, Recife, Brazil*, Lecture Notes in Bioinformatics (LNBI) 8213, pp. 1–11, Springer International Publishing, Switzerland.

Andronescu,M. *et al.* (2007) Efficient parameter estimation for RNA secondary structure prediction. *Bioinformatics*, **23**, i19–i28.

Angelbello,A.J. *et al.* (2018) Using genome sequence to enable the design of medicines and chemical probes. *Chem. Rev.*, **118**, 1599–1663.

Bellaousov,S. and Mathews,D.H. (2010) Probknot: fast prediction of RNA secondary structure including pseudoknots. *RNA*, **16**, 1870–1880.

Bernhart,S.H. *et al.* (2006) Local RNA base pairing probabilities in large sequences. *Bioinformatics*, **22**, 614–615.

Bringmann,K. *et al.* (2016) Truly sub-cubic algorithms for language edit distance and RNA-folding via fast bounded-difference min-plus product. In: *2016 IEEE 57th Annual Symposium on Foundations of Computer Science (FOCS) New Brunswick, NJ, USA*, IEEE, pp. 375–384.

Castanotto,D. and Rossi,J.J. (2009) The promises and pitfalls of RNA-interference-based therapeutics. *Nature*, **457**, 426–433.

Childs-Disney,J.L. *et al.* (2007) A small molecule microarray platform to select RNA internal loop-ligand interactions. *ACS Chem. Biol.*, **2**, 745–754.

Crooke,S. (2004) Antisense strategies. *Curr. Mol. Med.*, **4**, 465–487.

Dirks,R.M. and Pierce,N.A. (2003) A partition function algorithm for nucleic acid secondary structure including pseudoknots. *J. Comput. Chem.*, **24**, 1664–1677.

Do,C. *et al.* (2006) Contrafold: rNA secondary structure prediction without physics-based models. *Bioinformatics*, **22**, e90–e98.

Eddy,S.R. (2001) Non-coding RNA genes and the modern RNA world. *Nat. Rev. Genet.*, **2**, 919–929.

Frazier,L. and Rayner,K. (1982) Making and correcting errors during sentence comprehension: eye movements in the analysis of structurally ambiguous sentences. *Cogn. Psychol.*, **14**, 178–210.

Fu,Y. *et al.* (2015) Discovery of novel ncRNA sequences in multiple genome alignments on the basis of conserved and stable secondary structures. *PLoS One*, **10**, e0130200.

Gareiss,P.C. *et al.* (2008) Dynamic combinatorial selection of molecules capable of inhibiting the (CUG) repeat RNA-MBNL1 interaction in vitro: discovery of lead compounds targeting myotonic dystrophy (DM1). *J. Am. Chem. Soc.*, **130**, 16254–16261.

Gilbert,W. (1986) Origin of life: the RNA world. *Nature*, **319**, 618.

Gruber,A. *et al.* (2010) RNAz 2.0: improved noncoding RNA detection. In: *Pacific Symposium on Biocomputing*. Vol. **15**, World Scientific Publishing Co Pte Ltd, pp. 69–79.

Gultyaev,A.P. *et al.* (1995) The computer simulation of RNA folding pathways using a genetic algorithm. *J. Mol. Biol.*, **250**, 37–51.

Hofacker,I.L. and Lorenz,R. (2014) Predicting RNA structure: advances and limitations. In: Waldsich,C. (ed.), *RNA Folding: Methods and Protocols. Methods in Molecular Biology 1086*, pp. 1–19, Humana Press, Totowa, NJ, USA.

Huang,L. and Chiang,D. (2005) Better k-best Parsing. In: *Proceedings of the Ninth International Workshop on Parsing Technologies (IWPT-2005)*, Association for Computational Linguistics, pp. 53–64.

Huang,L. and Sagae,K. (2010) Dynamic programming for linear-time incremental parsing. In: *Proceedings of ACL. Uppsala, Sweden*. Association for Computational Linguistics, pp. 1077–1086

Huang,L. *et al.* (2012) Structured perceptron with inexact search. In: *Proceedings of NAACL 2012*, Association for Computational Linguistics, pp. 142–151.

Joyce,G.F. (1994) *In vitro* evolution of nucleic acids. *Curr. Opin. Struct. Biol.*, **4**, 331–336.

Kasami,T. (1965) An efficient recognition and syntax analysis algorithm for context-free languages. *Technical Report AFCRL-65-758*. AFCRL.

Kiryu,H. *et al.* (2008) Rfold: an exact algorithm for computing local base pairing probabilities. *Bioinformatics*, **24**, 367–373.

Lai,W.-J.C. *et al.* (2018) The formation of intramolecular secondary structure brings mRNA ends in close proximity. *Nat. Commun.*, **9**, 4328.

Lange,S.J. *et al.* (2012) Global or local? predicting secondary structure and accessibility in mRNAs. *Nucleic Acids Res.*, **40**, 5215–5226.

Leija-Martínez,N. *et al.* (2014) The separation between the 5'-3' ends in long RNA molecules is short and nearly constant. *Nucleic Acids Res.*, **42**, 13963–13968.

Li,T.J. and Reidys,C.M. (2018) The rainbow spectrum of RNA secondary structures. *Bull. Math. Biol.*, **80**, 1514–1538.

Licon,A. *et al.* (2010) A dynamic programming algorithm for finding the optimal segmentation of an RNA sequence in secondary structure predictions. In: *2nd International Conference on Bioinformatics and Computational Biology*. ACM, pp. 165–170

Lorenz,R. *et al.* (2011) ViennaRNA package 2.0. *Algorithms Mol. Biol.*, **6**, 1.

Lu,Z.J. and Mathews,D.H. (2008) Efficient siRNA selection using hybridization thermodynamics. *Nucleic Acids Res.*, **36**, 640–647.

Mathews,D.H. and Turner,D.H. (2006) Prediction of RNA secondary structure by free energy minimization. *Curr. Opin. Struct. Biol.*, **16**, 270–278.

Mathews,D.H. *et al.* (1999) Expanded sequence dependence of thermodynamic parameters improves prediction of RNA secondary structure. *J. Mol. Biol.*, **288**, 911–940.

Mathews,D.H. *et al.* (2004) Incorporating chemical modification constraints into a dynamic programming algorithm for prediction of RNA secondary structure. *Proc. Natl. Acad. Sci. USA*, **101**, 7287–7292.

McCaskill,J.S. (1990) The equilibrium partition function and base pair binding probabilities for RNA secondary structure. *Biopolymers*, **29**, 1105–1119.

Meyer,I.M. and Miklós,I. (2004) Co-transcriptional folding is encoded within RNA genes. *BMC Mol. Biol.*, **5**, 10.

Nussinov,R. *et al.* (1978) Algorithms for loop matchings. *SIAM J. Appl. Math.*, **35**, 68–82.

Palde,P.B. *et al*. (2010) Strategies for recognition of stem-loop RNA structures by synthetic ligands: application to the HIV-1 frameshift stimulatory sequence. *J. Med. Chem.*, **53**, 6018–6027.

Rastegari,B. and Condon,A. (2005). Linear time algorithm for parsing RNA secondary structure. In: *International Workshop on Algorithms in Bioinformatics, Mallorca, Spain*. Springer, pp. 341–352.

Reeder,J. and Giegerich,R. (2004) Design, implementation and evaluation of a practical pseudoknot folding algorithm based on thermodynamics. *BMC Bioinformatics*, **5**, 1.

Sato,K. *et al*. (2009) Centroidfold: a web server for RNA secondary structure prediction. *Nucleic Acids Res.*, **37**, W277–W280.

Sato,K. *et al*. (2011) Ipknot: fast and accurate prediction of RNA secondary structures with pseudoknots using integer programming. *Bioinformatics*, **27**, i85–i93.

Sazani,P. *et al*. (2002) Systemically delivered antisense oligomers upregulate gene expression in mouse tissues. *Nat. Biotechnol.*, **20**, 1228–1233.

Seetin,M.G. and Mathews,D.H. (2012) RNA structure prediction: an overview of methods. In: Keiler,K. (ed.) *Bacterial Regulatory RNA: Methods and Protocols*. Humana Press,Totowa, NJ, USA, pp. 99–122.

Sloma,M. and Mathews,D. (2016) Exact calculation of loop formation probability identifies folding motifs in RNA secondary structures. *RNA*, **22**, 1808–1818.

Stephens,Z.D. *et al*. (2015) Big data: astronomical or genomical? *PLoS Biol.*, **13**, e1002195.

Tafer,H. *et al*. (2008) The impact of target site accessibility on the design of effective siRNAs. *Nat. Biotechnol.*, **26**, 578–583.

The RNAcentral Consortium (2017) RNAcentral: a comprehensive database of non-coding RNA sequences. *Nucleic Acids Res.*, **45**, D128–D134.

Tomita,M. (1988) Graph-structured stack and natural language parsing. In: *Proceedings of ACL*. Association for Computational Linguistics, pp. 249–257.

Venkatachalam,B. *et al*. (2014) Faster algorithms for RNA-folding using Four-Russians method. *Algorithms Mol. Biol.*, **9**, 5.

Washietl,S. *et al*. (2012) Computational analysis of noncoding RNAs. *Wiley Interdiscip. Rev. RNA*, **3**, 759–778.

Watters,K.E. *et al*. (2016) Cotranscriptional folding of a riboswitch at nucleotide resolution. *Nat. Struct. Mol. Biol.*, **23**, 1124.

Watts,J.M. *et al*. (2009) Architecture and secondary structure of an entire HIV-1 RNA genome. *Nature*, **460**, 711–716.

Yoffe,A.M. *et al*. (2011) The ends of a large RNA molecule are necessarily close. *Nucleic Acids Res.*, **39**, 292–299.

Younger,D.H. (1967) Recognition and parsing of context-free languages in time n^3. *Inf. Control*, **10**, 189–208.

Zakov,S. *et al*. (2011) Reducing the worst case running times of a family of RNA and CFG problems, using valiant's approach. *Algorithms Mol. Biol.*, **6**, 20.

Zhao,Y. *et al*. (2016) Noncode 2016: an informative and valuable data source of long non-coding RNAs. *Nucleic Acids Res.*, **44**, D203–D208.

Zuker,M. and Stiegler,P. (1981) Optimal computer folding of large RNA sequences using thermodynamics and auxiliary information. *Nucleic Acids Res.*, **9**, 133–148.

Zuker,M. *et al*. (1991) A comparison of optimal and suboptimal RNA secondary structures predicted by free energy minimization with structures determined by phylogenetic comparison. *Nucleic Acids Res.*, **19**, 2707–2714.